объединенный
институт
ядерных
исследований
дубна

E4-93-334

V.Yu.Ponomarev, V.V.Voronov

LOOKING INSIDE GIANT RESONANCE FINE STRUCTURE

Invited talk at the «Gull Lake Nuclear Physics Conference on Giant Resonances» (Gull Lake, U.S.A. 17—21 August 1993)

1993

1. INTRODUCTION

During a many-year history of investigation of giant resonances a lot of information on their properties has been gained [1,2]. The present experimental development of the coincidence technique allows one to consider in detail some specific properties of giant resonances like their γ- and particle-decay. By different measurements we may separate information on different states contributing to giant resonances in non-coincidence experiments and thus look inside the resonance structure. Another source of information on the fine structure of giant resonances is inelastic scattering experiments with a high resolution. We can mention here (e,e') experiments [3] or recent (p,p') measurements below the particle threshold which distinguish fragmentation of a resonance in a group of many discrete states [4]. These experimental achievements demand theoretical treatment of giant resonances on an equivalent level. One of them will be presented here.

2. FORMALISM AND DETAILS OF CALCULATIONS

Microscopic analysis of states forming giant resonances as well as low-lying states has been performed within the Quasiparticle Phonon Model (QPM) [5-7]. The model Hamiltonian $\mathcal{H}$ includes an average field $V_{p(n)}$ for protons and neutrons, a monopole pairing interaction and isoscalar and isovector residual interaction of a separable type with a form factor proportional to $dV_{p(n)}/dr$. Excited states of even-even nuclei are treated in terms of phonon excitations built upon the ground state that is considered as a phonon vacuum $|0>_{ph}$. Phonon creation operator $Q^+_{\lambda\mu i}$ for multipolarity $\lambda\mu$ is introduced as a linear combination of two quasiparticle creation α^+_{jm} and annihilation α_{jm} operators with the shell quantum numbers jm of the average field V as follows:

$$Q^+_{\lambda\mu i} = \frac{1}{2}\sum_{j\,j'}^{p,n}\{\psi^{\lambda i}_{jj'}[\alpha^+_{jm}\alpha^+_{j'm'}]_{\lambda\mu} + (-1)^{\lambda-\mu}\phi^{\lambda i}_{jj'}[\alpha_{jm}\alpha_{j'm'}]_{\lambda-\mu}\} \quad , \tag{1}$$

where

$$[\alpha^+_{jm}\alpha^+_{j'm'}]_{\lambda\mu} = \sum_{mm'} < jmj'm'|\lambda\mu > \alpha^+_{jm}\alpha^+_{j'm'} \ .$$

The forward $\psi^{\lambda i}_{jj'}$ and backward $\phi^{\lambda i}_{jj'}$ amplitudes are obtained by solving RPA equations that yield a set of one-phonon configurations with excitation energies $\omega_{\lambda i}$ and RPA root number i. Among phonons we obtain both collective and practically pure two-quasiparticle excitations.

We assume that mixing of one-phonon configurations, through which giant resonances are excited in inelastic scattering, with more complex configurations is sufficiently strong in the resonance region. Thus, we write the wave function of resonance states as a sum of configurations of different complexity by the number of phonons. If we limit this sum to one- and two-phonon configurations only, the wave function for the λ^π_ν-state has the form:

$$\Psi_\nu(\lambda\mu) = \{\sum_i R_i(\lambda\nu)Q^+_{\lambda\mu i} + \sum_{\lambda_1 i_1 \lambda_2 i_2} P^{\lambda_2 i_2}_{\lambda_1 i_1}(\lambda\nu)\left[Q^+_{\lambda_1\mu_1 i_1}Q^+_{\lambda_2\mu_2 i_2}\right]_{\lambda\mu}\}|0>_{ph} \ . \qquad (2)$$

In actual calculations we do not include two-phonon configurations made of both non-collective phonons for the second term of the wave function (2). By this truncation of the two-phonon basis, we remove complex configurations that are weakly coupled to one-phonon states and, on the other hand, may strongly violate the Pauli principle.

For the amplitudes $R_i(\lambda\nu)$ and $P^{\lambda_2 i_2}_{\lambda_1 i_1}(\lambda\nu)$, eq. (2), we diagonalize the model Hamiltonian on the basis of wave functions (2). Eigenvalues E_ν of states (2) are got as the roots of the following determinant:

$$F(E_\nu) = det|(\omega_{\lambda i} - E_\nu)\delta_{ii'} - \frac{1}{2}\sum_{\lambda_1 i_1, \lambda_2 i_2} \frac{U^{\lambda_2 i_2}_{\lambda_1 i_1}(\lambda i)U^{\lambda_2 i_2}_{\lambda_1 i_1}(\lambda i')}{\omega_{\lambda_1 i_1} + \omega_{\lambda_2 i_2} - E_\nu}| = 0 \ , \qquad (3)$$

where

$$U^{\lambda_2 i_2}_{\lambda_1 i_1}(\lambda i) = < Q_{\lambda i}||\mathcal{H}||\left[Q^+_{\lambda_1 i_1}Q^+_{\lambda_2 i_2}\right]_\lambda >$$

is the matrix element of interaction between one- and two-phonon configurations which is a function [6] of the amplitudes $\psi^{\lambda i}_{jj'}$ and $\phi^{\lambda i}_{jj'}$, eq. (1) and thus, calculated

microscopically as soon as a phonon basis is fixed. The rank of the determinant (3) is determined by the number of one-phonon configurations included in the first term of the wave function (2).

Numerical calculations have been performed with the Woods-Saxon potential for an average field with the parameters from ref. [8]. Parameters of the residual interactions were adjusted to the properties of the low-lying collective levels. Natural parity phonons with $\lambda^\pi = 1^-$ - 8^+ have been included in the two-phonon term of the wave function (2).

3. SOME RESULTS

With a complete information on the fine structure of giant resonances obtained in this way, we may consider different physical processes in which different states from the resonance region are excited by different probes, and in coincidence technique of measuring decay properties of these states, fingerprints of some specific states from the resonance region can be observed. This allows one to consider giant resonances not as broad featureless structures but as a set of a great number of states with their own properties and also serves as a good test for existing nuclear models.

3.1. Fine structure of the GDR

First, let us demonstrate the fragmentation of the B(Eλ) strength due to the coupling of one-phonon configurations to two-phonon ones in the resonance region. We take as an example the giant dipole resonance (GDR) in ^{136}Xe. The top part of Figure 1 presents the B(E1) strength distribution over one-phonon configurations. The major part of the B(E1) strength is carried by these configurations, the direct excitation of two-phonon 1^- states from the ground state is about three orders of magnitude weaker. The coupling of simple (one-phonon) configurations to more complex (two-phonon) ones results in a strong fragmentation of one-phonon states over the states with the wave function (2),the bottom part of Figure 1. This example clearly shows how the width of a giant resonance appears. Calculations on the set of wave functions, eq. (2), somewhat underestimate within a few hundred of keV the experimentally measured widths of giant resonances. This is not surpris-

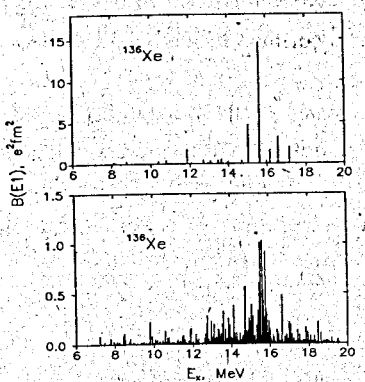

Figure 1: *GDR in ^{136}Xe. E1-strength distribution over one-phonon configurations (top). Coupling to complex configurations, wave function, eq. (2), is allowed for (bottom).*

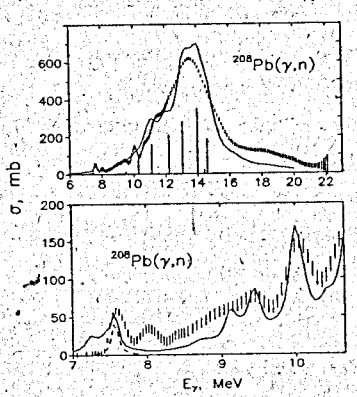

Figure 2: *Experimental and theoretical $(\gamma,n)^{208}Pb$ cross section. Calculations are performed with Δ = 1 MeV (top) and 0.2 MeV (bottom).*

ing since configurations more complex than two-phonon ones are not included. To achieve better agreement with an experiment in the B(Eλ) strength distribution, an additional artificial damping width, which effectively simulates truncated complex configurations, is included by using the well-known strength function method.

3.2. Substructures of the (γ,n)Pb cross section

Some substructures of the GDR have been observed in the (γ,n) cross sections at low excitation energies [9]. The experimental $(\gamma,n)^{208}$Pb cross section is presented in the top part of Figure 2. It is compared to the calculated energy averaged cross section of the dipole photon adsorption

$$\sigma_{\gamma\prime}(E_\gamma) = 4,025\, E_\gamma\, b(E1,E_\gamma)\ , \tag{4}$$

where

$$b(E1,E) = \sum |<\nu||M(E1)||0>|^2\, \frac{1}{2\pi}\, \frac{\Delta}{(E-E_\nu)^2+\Delta^2/4} \tag{5}$$

is the strength function of the dipole strength distribution calculated with the artificial damping parameter Δ = 1 MeV. One can see from Figure 2 a rather good agreement of experimental data with the theoretical calculations for the photoneutron cross section. Some overestimation of a cross section near a maximum and underestimation of a high energy part in our calculation are caused by the truncation of a large number of two phonon configurations which are weakly coupled with one-phonon states. An integral contribution of these components may be essentially taken into account by increasing the energy averaging parameter Δ. The results of the RPA calculation for the dipole strength distribution are shown in the same figure by vertical lines. As can be seen from Figure 2, there are substructures in the low energy part of the cross section. They are located near the RPA collective states. The coupling of the last with the two-phonon states results in a redistribution of the dipole strength. For the low energy part where a level density is not so high substructures are pronounced. The increasing of the excitation energy leads to increasing of the level density, and as a result, substructures disappear. One cannot observe any substructures in nuclei with open shells because of the high level densities and strong coupling between configurations [10].

To shed more light on the problem of the substructure existence, the low energy part of the cross section with smaller Δ =0.2 MeV has been calculated. The results of calculations are given in the bottom part of Figure 2. Our calculations reproduce the main structures observed by the experiment at the excitation energies 7.6, 8.6, 9.1, 9.5, 10.0 and 11.3 MeV. The substructure at the energy 7.6 MeV is formed by E1– and M1(dashed line)–transitions. As can be seen from the bottom part of Figure 2, the isovector M1–resonance contributes essentially to the cross section in this energy region. This result is in good agreement with the experimental M1 strength distribution which has been measured with highly polarized tagged photons [11]. We fail to reproduce the substructure at the energy 8 MeV, nevertheless, there is a two–bump structure in the calculated absorption cross section at lower energies. Some disagreement between calculations and experimental data may be caused apparently by inaccuracies of our single particle energies but we did not try to get an ideal description of experimental data. It is worth mentioning that E2–transitions do not give any noticeable contribution to the cross section.

3.3. γ-decay of the GDR into the ground and 2_1^+ states

Recently, ^{116,124}Sn$(\alpha,\alpha'\gamma)$ experiments have been performed at the KVI [12]. The GDR region of excitation was investigated. Coincidence measurements between the scattered α-particles and the emitted γ-rays were used to select the contribution of the GDR from the giant monopole (GMR) and quadrupole (GQR) resonances. It was observed that the population of the first 2^+ excited state in tin isotopes was nearly as strong as the ground state. The following idea of interpreting the results of these experiments has been proposed [13]. As soon as the GDR is excited by α particles, it decays into the ground state by E1 transitions. Since the γ-decay into the 2_1^+ state is strong, it might mean that the coupling of the GDR with two-phonon configurations $[GDR \otimes 2_1^+]_{1^-}$ is sufficiently strong, and we observe E1 transitions from these two-phonon configurations to the first 2^+ state. To consider γ-decay into the 2_1^+ state, we need to know the structure of each 1^- state contributing to the GDR. Thus, the fine structure of the GDR has been calculated.

The ideas of the multistep theory of nuclear reactions (see e.g. [14]) have applied in the calculation of the $(\alpha,\alpha'\gamma)$ cross sections, and the $\sigma_{\dot{a},\alpha'\gamma}(E)$ coincidence cross section has been deduced following the procedure described in ref. [15] as:

$$\sigma_{\alpha,\alpha'\gamma}(E) = \sigma_{\alpha,\alpha'}(E)\left[\frac{\Gamma_\gamma(E)}{\Gamma} + \frac{\Gamma^\downarrow}{\Gamma}B_{CN}(E)\right], \qquad (6)$$

where $\Gamma_\gamma(E)$ is the width of the γ-decay of an intermediate 1^- state into the ground or the 2_1^+ state and Γ is the GDR width. The second term in eq. (6) corresponds to the compound decay.

Using the calculated structure of the 1^- states in the GDR region we can obtain microscopically both the cross section of excitation $\sigma_{\alpha,\alpha'}(E_{1^-\nu})$ of each ν^{th} 1^- state and its decay width into the ground state or the 2_1^+ state. The GDR excitation at the KVI energies is dominated by the Coulomb term. Thus, we can approximate the form factor of excitation of the i^{th} one-phonon 1^- configuration by electromagnetic matrix elements $< 1_i^- \parallel E1 \parallel 0_{gs}^+ >$ multiplied by the energy-dependent part of the excitation cross section. The decay width $\Gamma_\gamma(E_{1^-\nu})$ of the ν^{th} 1^- excited state in eq. (6) is simply related to the γ-transition matrix elements between one-phonon configurations and the phonon vacuum for the decay into the ground

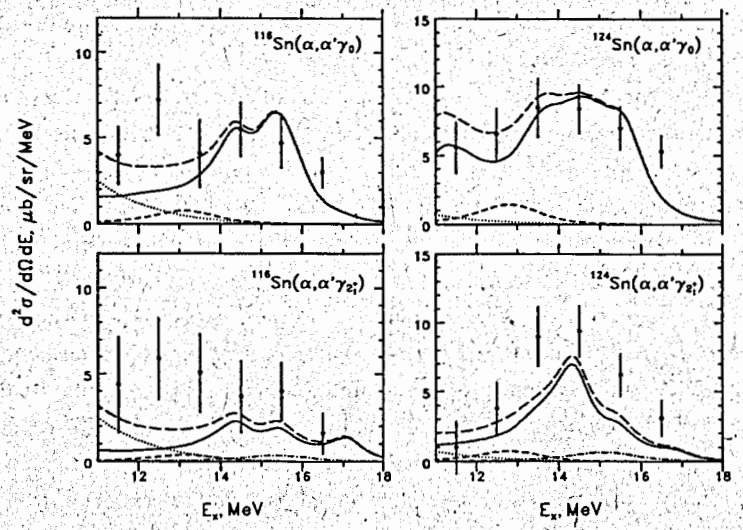

Figure 3: *Measured differential cross section for inelastic α-scattering in coincidence with γ decay into the ground state (top) and the 2_1^+ state (bottom) of ^{116}Sn and ^{124}Sn as a function of excitation energy in comparison with the QPM calculations. Solid line corresponds to the excitation of the GDR; dashed line – the GQR; dot-dashed line – the GMR; dotted line is a contribution of the compound decay and long-dashed line is the sum of all contributions.*

state and between two-phonon and one-phonon configurations for the decay into the 2_1^+ state. The calculated cross sections have been averaged with the averaging parameter $\Delta = 1$ MeV equal to the bin size used in experimental data.

The calculated cross sections corresponding to the excitation and decay of the GDR are presented in Figure 3 by the solid lines. The exponential dependence of the Coulomb excitation cross section as a function of excitation energy strongly enhances lower energies. As a result, the maximum in the $\sigma_{\alpha,\alpha'\gamma_0}(E)$ cross sections is shifted down compared to the E1 strength distribution. Contributions to the total $\sigma_{\alpha,\alpha'\gamma_0}(E)$ cross sections from excitation and decay of the GQR (dashed lines in Figure 3) at lower energies has been estimated phenomenologically as well as the contribution from the GMR (dot-dashed lines) for the decay into 2_1^+ state.

The dotted lines are the contribution from the compound decay and the resulting cross sections are presented by long dashed lines.

The shape of the $\sigma_{\alpha,\alpha'\gamma_0}(E)$ cross sections is described rather well without introducing any artificial width of the GDR although the point at 12.5 MeV in $\sigma_{\alpha,\alpha'\gamma_0}(E)$ for ^{116}Sn is not reproduced in the calculation. The shape of the $\sigma_{\alpha,\alpha'\gamma_{2_1^+}}(E)$ cross section is very sensitive to the coupling of the GDR with the GDR built on the first 2^+ state. If the coupling is weak, these two modes exist independently with centroids separated by the energy of the 2_1^+ state. In this case, the $(\alpha,\alpha'\gamma_{2_1^+})$ cross section is very small. By increasing the coupling we can expect two maxima in the $\sigma_{\alpha,\alpha'\gamma_{2_1^+}}(E)$ cross section from the two afore-mentioned modes, with the one at higher energy suppressed by the Coulomb factor. This coupling is determined by the collectivity of both the first 2^+ state and the GDR. To reproduce the collectivity of the 2_1^+ state, the parameter of the isoscalar quadrupole residual interaction has been adjusted to obtain in the calculation the experimental value of the B(E2, $2_1^+ \rightarrow 0_{g.s.}^+$) transition [16]. The collectivity of the 2_1^+ state in ^{116}Sn is somewhat stronger as compared to the one in ^{124}Sn [16]. It results in a wider distribution of $\sigma_{\alpha,\alpha'\gamma_{2_1^+}}(E)$ in ^{116}Sn (see solid lines in the bottom of Figure 3).

The shape of the $\sigma_{\alpha,\alpha'\gamma_{2_1^+}}(E)$ cross sections peaking around 14.5 MeV in ^{124}Sn and practically flat in ^{116}Sn is reproduced, in general, by the QPM calculations although the amplitudes of these cross sections are underestimated. The ratio of the energy integrated $(\alpha,\alpha'\gamma_0)$ and $(\alpha,\alpha'\gamma_{2_1^+})$ cross sections over the energy interval 12-17 MeV can be estimated from the experiment as 1.5±0.5 for ^{116}Sn and 1.1±0.3 for ^{124}Sn. The calculation gives the values 2.1 and 2.0, respectively. It should be mentioned that different shapes of the $\sigma_{\alpha,\alpha'\gamma_0}(E)$ and $\sigma_{\alpha,\alpha'\gamma_{2_1^+}}(E)$ cross sections from both experiment and calculation support the assumption of a sufficiently strong mixing between the GDRs built on the ground and 2_1^+ states.

3.4. γ decay of the HEOR

The idea that giant resonance states can be excited via one-phonon configurations and then decay by means of two-phonon configurations of their wave functions can be applied to investigation of giant resonances of high multipolarity for which γ-decay to the ground state is strongly suppressed. As an example, we consider γ-decay properties of the High Energy Octupole Resonance (HEOR) in

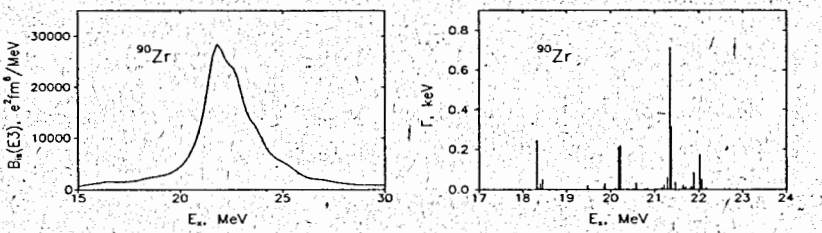

Figure 4: *Calculated strength function of the isoscalar E3 strength distribution in the HEOR region (left) and γ decay widths of the HEOR to low-lying 2^+ and 4^+ states (right) in ^{90}Zr.*

^{90}Zr. It may be excited by some isoscalar probe and the corresponding, calculated within the QPM, strength function is presented in the left part of Figure 4. In this calculation, the HEOR has the energy centroid $E_x = 22.4$ MeV and the total width $\Gamma = 4.4$ MeV.

Because of the high density of two-phonon configurations in the HEOR region we have succeeded in calculating the HEOR γ-decay into the low-lying collective $2_{1,4}^+$ and $4_{1,2}^+$ states only on the truncated two-phonon basis. The partial γ-decay widths for these transitions calculated under the assumption of isoscalar nature of the HEOR excitation are shown in the right part of Figure 4. The total width $\Gamma_{HEOR\rightarrow 2_{1,4}^+,4_{1,2}^+}$ is equal to 3 keV or about 10% of the GDR γ-decay width into the ground state. It opens a new possibility to investigate the HEOR.

4. CONCLUSIONS

The Quasiparticle Phonon Model has been applied here to calculations of the fine structure of giant resonances. The model Hamiltonian has been diagonalized on the basis of the wave functions of excited states which include one- and two-phonon configurations. A complete information on the wave function of each state contributing to a giant resonance allows one to consider the decay properties of the resonance into the ground and low-lying excited states. As an example, the γ-decay of the GDR into the first 2^+ state and the HEOR into the low-lying 2^+ and 4^+ states have been presented.

REFERENCES

1. K. Goeke and J. Speth , Ann. Rev. Nucl. Part. Sci. **32** (1982) 65.
2. A. van der Woude, Electric and Magnetic Giant Resonances in Nuclei, ed. J. Speth, World Scientific Publishing Company (1991) 99.
3. G. Kilgus et al., Z.Phys. **A326** (1987) 41.
4. Y. Fujita et al., Phys. Rev. **C40** (1989) 1595.
5. A.I. Vdovin and V.G. Soloviev, Particles and Nuclei **14** (1983) 237.
6. V.V. Voronov and V.G. Soloviev, Particles and Nuclei **14** (1983) 1380.
7. V.G. Soloviev, Prog. in Part. and Nucl. Phys. **17** (1987) 107.
8. V.Yu. Ponomarev et al., Nucl. Phys. **A323** (1979) 446.
9. S.N. Belyaev et al., Sov. Journ. of Nucl. Phys. **55** (1992) 157.
10. V.G. Soloviev et al., Nucl. Phys. **A304** (1978) 503.
11. R.M. Laszewski et al., Phys. Rev. Lett. **61** (1988) 1710.
12. A. Krasznahorkay et al., Phys. Rev. Lett. **66** (1991) 1287.
13. V.Yu. Ponomarev and A. Krasznahorkay, Nucl. Phys. **A550** (1992) 150.
14. H. Feshbach, A. Kerman and S. Koonin, Ann. Phys. (N.Y.) **125** (1980) 429.
15. J.R. Beene et al., Phys. Rev. **C41** (1990) 920.
16. P.M. Endt, Atomic data and nucl. data tables **26** (1981) 47.

Received by Publishing Departmen
on September 8, 1993.